Carbohydrate Polymers 331 (2024) 121842

Contents lists available at ScienceDirect

Carbohydrate Polymers

journal homepage: www.elsevier.com/locate/carbpol

Development of acid-free chitosan films in food coating applications: Provolone cheese as a case study

Roberto Casalini [a], Filippo Ghisoni [a], Lorenzo Bonetti [a], Andrea Fiorati [a,b,*], Luigi De Nardo [a,b]

[a] Department of Chemistry, Materials, and Chemical Engineering "G. Natta" Politecnico di Milano, Piazza Leonardo da Vinci 32, I-20133 Milano, Italy
[b] INSTM, Local Unit Politecnico di Milano, Piazza Leonardo da Vinci 32, I-20133 Milano, Italy

ARTICLE INFO

Keywords:
Acid-free chitosan
Cheese preservation
Coating
Food safety
Food packaging
Shelf life

ABSTRACT

Chitosan has been extensively explored in food coatings. Still, its practical application is largely hampered by its conventional wet processing in acetic acid, whose residuals negatively impact food quality and safety. Here, we propose a new method to formulate chitosan coatings for food applications by avoiding organic acid processing and validate them on a cheese model. The procedure entails modifying a previously reported process based on HCl chitosan treatment and neutralising the resulting gel. The obtained chitosan is solubilised in water using carbonic acid that forms in situ by dissolving carbon dioxide gas. The reversibility of water carbonation allows for easy removal of carbonic acid residues, resulting in acid-free chitosan films and coatings. The performance of the coating was tested against state-of-the-art chitosan-based and polymeric coatings. We preliminarily characterised the films' properties (water stability, barrier, and optical properties). Then, we assessed the performance of the coating on Provolone cheese as a food model (mass transfer and texture profiles over 14 days). The work demonstrated the advantage of the proposed approach in solving some main issues of food quality and safety, paving the way for an effective application of chitosan in future food contact applications.

1. Introduction

The modern food industry relies on oil-based polymers to realise packaging solutions that preserve food and extend shelf life (Mohamed et al., 2020). Despite the relatively low cost, easy processing, and favourable properties of conventional plastics (Otoni et al., 2017), increasing concerns about using non-renewable sources and limited end-of-life options have fuelled a growing interest in bio-based polymers (Amulya et al., 2021). Numerous studies focused on proteins, lipids, and polysaccharides as raw materials for edible and compostable packaging, enabling advanced preservation approaches (Rao, 2023). Interestingly, these materials are often cost-effective and can be derived from agri-food industry by-products or wastes (Cazòn, 2017).

In this panorama, the ability of polysaccharides to enhance the quality, safety, and functionality of coated food has led to the development of several innovative food products (Paulo et al., 2021). Polysaccharides can form homogeneous films that prevent moisture and aroma loss, regulate solute transport, control water absorption, and limit oxygen permeation because of their well-ordered hydrogen-bonded network (Gennadios et al., 1997; Kocira et al., 2021; Ruggeri et al., 2021). Namely, chitosan-based coatings and films have been tested on several kinds of cheese to reduce microbiological growth and extend their shelf life (Cano Embuena et al., 2017; Elsabee & Abdou, 2013; Iqbal et al., 2021).

All these works process chitosan via wet techniques by exploiting its solubility in an acidic medium, primarily acetic acid (1–2 % v/v). Some precautions should be taken due to the acidic medium in which chitosan must be dissolved and the potential migration of the acid inside the food matrix. Volatile organic acids, such as acetic acid, are typically eliminated during solvent evaporation, but residual amounts may persist. Indeed, the European Commission regulates the amount of acetic acid that can migrate into a food product, generally at a threshold lower than 60 ppm (Reg 10/2011 EU, 2011). A pungent odour and taste also characterise acetic acid, its residuals impairing the product's organoleptic characteristics (Warmke et al., 1996). This pungent odour can be detected even at low concentrations, being the odour detection limit in the 0.006–0.135 ppm range (Nagata, 2012; Vera et al., 2020).

To overcome these issues, literature reports several approaches to neutralise the acidic residues, employing strong bases, such as sodium hydroxide (NaOH) (Chang et al., 2019; Takara et al., 2015). The

* Corresponding author at: Department of Chemistry, Materials, and Chemical Engineering "G. Natta" Politecnico di Milano, Piazza Leonardo da Vinci 32, I-20133 Milano, Italy.
E-mail address: andrea.fiorati@polimi.it (A. Fiorati).

https://doi.org/10.1016/j.carbpol.2024.121842
Received 6 October 2023; Received in revised form 15 January 2024; Accepted 18 January 2024
Available online 29 January 2024

neutralisation of coatings and films is usually obtained by immersion in an alkaline solution. However, such an approach could fail to remove all the residual acid, resulting in salt formation or residual excess of the base. In addition, it is characterised by long kinetics and a complex two-step procedure.

To overcome these limitations, an alternative approach to chitosan dissolution was originally proposed by Sakai and colleagues (Sakai et al., 2001, 2002). The authors reported obtaining homogeneous chitosan solutions by a preliminary dissolution in an acidic medium (HCl) followed by its neutralisation and complete removal of the formed salts. The obtained chitosan-based compact hydrogel can then be easily dissolved in water at atmospheric pressure by the carbonic acid (H_2CO_3) in situ formed through carbon dioxide (CO_2) dissolution. The reversibility of the process allows the easy removal of the acidic residues during the filming process, resulting in acid-free chitosan films (Sakai et al., 2001, 2002).

Despite the potential of this innovative approach (Zhang et al., 2018), acid-free chitosan films were poorly characterised. Moreover, this chitosan dissolution approach has only been applied in a limited number of applications, such as coating for cellulose-based materials (Sakai et al., 2002) and porous composites for biomedical applications (Gorczyca et al., 2014; Zhang et al., 2018). Approaches involving high-pressurized CO_2 were recently developed, even at supercritical conditions. However, the need for an apparatus to manage high pressure (up to 30 MPa) may hinder practical uses (Novikov et al., 2018; Otake et al., 2006). Hence, employing acid-free chitosan films may represent an easy approach to overcoming the issues the organic acids commonly employed in chitosan dissolution pose.

This research aims to develop an innovative acid-free chitosan coating that overcomes the limitations of food-contact chitosan applications, such as residual processing acid within the coating, low water stability, and poor moisture barrier properties. Obtained coatings were tested on a semi-hard cheese, *Provolone*, a member of the *Pasta Filata* family (Fox et al., 2017), which was chosen as the product model. The effectiveness of the acid-free coating was proved in comparison with the state-of-the-art chitosan and polymeric coatings, evaluating the mass variation in time and organoleptic properties of coated Provolone samples for 14 days. To gain further insights into the behaviour of the developed coatings, acid-free chitosan films were preliminarily characterised in terms of water stability, barrier, and optical properties.

2. Materials and methods

2.1. Materials

Chitosan (CS) powder (75 % deacetylated; medium molecular weight; viscosity 1 % in acetic acid 1 % 208 cP; Lot # STBF3507V), glycerol anhydrous >99.0 %, hydrochloric acid, glacial acetic acid (AcOH), and sodium hydroxide were purchased from Sigma-Aldrich (St Louis, MO, USA). CS characteristics were determined by the supplier and can be accessed by readers on the supplier's website using the lot number. A polyvinyl acetate (PVAc) based emulsion commonly used for cheese coatings (Parafluid neutro, FL 8063-180D) was kindly provided by *Università Cattolica del Sacro Cuore di Cremona*. Evonik Industries AG, Essen Germany, kindly provided Dynasylan F2815. Carbon dioxide (CO_2, E290, food grade) was bought in a pressurized steel cylinder (p = 6 MPa, T = 28 °C). All reagents were used without further purification. "Provolone Dolce" cheese samples were purchased from local grocery stores.

2.2. General procedure for film-forming solutions

The solution for acid-free coatings and films was prepared by adapting the procedure developed by Sakai and co-workers (Sakai et al., 2001, 2002). Chitosan (2.5 % w/v) was dissolved in a hydrochloric acid aqueous solution (0.15 M) at room temperature. The solution was neutralised with NaOH (0.5 M) under magnetic stirring until a pH > 7 was reached. The obtained hydrogel was collected by centrifugation (4000 rpm, 3 min). The hydrogel was washed with deionised water and centrifuged to separate the gel from the water until the rinse water reached a conductivity level lower than 80 μS (CM 35 conductivity meter CM35, cell 50 60). At the end of the process, the chitosan content was gravimetrically determined by drying an aliquot of the hydrogel.

The gel was dissolved by adding CO_2 gas at atmospheric pressure, dispersing the hydrogel in deionised water to achieve the final concentration (Table 1). An ice bath was used to increase the solubility of CO_2 within the solution. As a control, chitosan was dissolved in aqueous acetic acid (0.7–1.6 % v/v) solution by stirring it for 24 h at room temperature (Table 1). To improve the mechanical properties of films and coatings, glycerol (10 % w/w on chitosan mass basis, w/w_{cs}) was used as a plasticiser and added at the end of the dissolution process. Only plasticised materials were used for the cheese coating process. Table 1 summarises the different acronyms for films and coatings and the related solutions. (Fig. S1 reports pictures of the different solutions containing glycerol.)

Table 1
Composition of different solutions used to obtain films and coatings.

Acronyms	Dry matter	Dissolving solution	pH	Conductivity
	[%w/v]	[%v/v]	[−]	[μS]
Film				
CA[a]	Chitosan 2 %	AcOH 0.7 %	4.4	2.61×10^3
CAG[a]	Chitosan 2 % Glycerol 0.2 %	AcOH 0.7 %	4.6	2.52×10^3
CC	Chitosan 1.4 %	CO_2 [−]	5.7	5.8
CCG	Chitosan 1.4 % Glycerol 0.14 %	CO_2 [−]	5.6	65.8
PVAc	PVAc 45 %	–	4.2	4.07×10^3
Coating				
CA[a]	–	–	–	–
CAG[a]	Chitosan 4 % Glycerol 0.4 %	AcOH 1.6 %	5.1	4.38×10^3
CC	–	–	–	–
CCG	Chitosan 2 % Glycerol 0.2 %	CO_2 [−]	5.6	37.5
PVAc	PVAc 45 %	–	4.2	4.07×10^3

[a] CA and CAG film or coatings neutralised with NaOH (1 M) for 30 s and rinsed in deionised water for 10 s are defined as CA-N and CAG-N.

2.3. Rheological characterisation of the solutions

The rheological characterisation of the solutions was carried out with a rotational rheometer (MCR 302, Anton Paar, Italy) equipped with a parallel plate geometry (Ø = 25 mm), setting the working gap to 0.25 mm. Viscosity curves (viscosity (η) vs. shear rate ($\dot{\gamma}$)) were obtained after a preconditioning step ($\dot{\gamma} = 1000\ s^{-1}$ for 10 s, $\dot{\gamma} = 0.1\ s^{-1}$ for 30 s) in the shear rate range 0.1–1000 s^{-1}. The temperature dependence of the viscosity for each solution was investigated at T = 4, 16, and 37 °C. Tests were performed in triplicate (n = 3) and fitted at a fixed shear rate with an Arrhenius-like equation (Eq. (1)) (El-Hafian et al., 2010):

$$\eta = A^* e^{-\frac{E_a}{R*T}} \quad (1)$$

where A is the pre-exponential Arrhenius factor, E_a is the activation energy, R is the perfect gas constant (8.314 J mol^{-1} K^{-1}), and T is the absolute temperature in K.

2.4. Film preparation

Chitosan films were obtained via solvent casting: the solutions were poured into borosilicate glass Petri dishes (diameter = 10 cm). To improve the flexibility of the films for coating application, adding 10 %

w/w_{cs} glycerol was considered, resulting in easier extraction from the casting moulds and handling of the dry films. Moreover, to facilitate the peeling phase of the dried film, Petri dishes were treated with Dynasylan (F2815, Evonik Industries AG, Essen, Germany) by wetting the entire surface of each Petri dish (100 μL) followed by a drying period (24 h, 37 °C). Chitosan solutions (Table 1) were poured into the Petri dishes and dried at room temperature for 72 h. Before drying, the poured acid-free solution was degassed under a vacuum (−1 bar, 1 min) to avoid bubble formation. After the drying phase, some acetic acid-containing samples (defined as CA-N and CAG-N) were immersed in $NaOH_{1M}$ solution for 30 s to neutralise the acid still present in the film and then rinsed in deionised water for 10 s to remove salts and the excess of $NaOH_{1M}$. The films were then dried for 3 h at room temperature. All the prepared films were then conditioned at 37 °C, 0 % RH for at least 7 days before characterisation.

2.5. Film characterisation

2.5.1. Water stability

Swelling tests were performed by submerging chitosan films ($n = 3$ per film type) in PBS (phosphate buffer saline, pH 7.4) inside multiwell plates at 37 °C (weight = 34 ± 7 mg, volume = 29 ± 2 mm^3). The chitosan films were carefully removed and weighed for up to 24 h or until the absorption plateau was reached. The swelling ratio (SR) at timepoint t was computed using Eq. (2).

$$SR_t[\%] = \frac{W_t - W_0}{W_0} * 100 \tag{2}$$

where W_t is the mass of the swollen sample at time-point t [g] and W_0 the initial mass of the sample [g].

2.5.2. Barrier properties

The water vapour transmission rate (WVTR) was assessed by the dry cup method, according to the ASTM E96-22 standard. The permeation cups (VF2200, TQC, The Netherlands) were filled with dry calcium chloride as a desiccant to achieve an internal 0 % relative humidity (RH). Subsequently, the chitosan films (n = 3 per film type) were sealed on the permeation cups, and the cups were stored at T = 37 °C, RH = 100 %. Weight measurements were regularly acquired at stationary conditions: the slope (W) of the weight gain vs. time curves was determined by linear regression. The WVTR was then calculated using Eq. (3):

$$WVTR = \frac{W}{A} \left[\frac{g}{m^2\ d}\right] \tag{3}$$

where A is the permeation area of the cups [m^2], and W the weight gain's slope against time [g d^{-1}]. As the samples have different thicknesses, the comparison was made on water vapour permeability (WVP). The calculation for WVP is shown in Eq. (4).

$$WVP = \frac{WVTR}{P^0_{H_2O} * \Delta Rh} * th \left[\frac{g\ mm}{m^2\ d\ Pa}\right] \tag{4}$$

where $P^0_{H_2O}$ is the water saturation pressure [Pa], ΔRh the difference of relative humidity across the films [−], and th the thickness of the sample [mm].

The oxygen transmission rate (OTR) was determined following the ASTM D 3985–17 standard, using a stainless-steel permeation cell equipped with an oxygen sensor (PSt6 PreSens, Germany) and an optical reader (Fibox 4, PreSens, Germany). The cell features two chambers, and the films ($n = 3$ per film type) to be tested were securely fixed between the chambers using vacuum grease. Nitrogen was initially flushed through both cell chambers to ensure the absence of oxygen and to detect any leaks. Pure oxygen (RH 0 %) was purged into the lower chamber, and measurements were taken over 96 h.

The slope of the oxygen concentration versus time curves was determined using linear regression. The OTR was subsequently calculated according to the Eq. (5):

$$OTR = \frac{\dot{P}_{O_2} * V}{P_{Std} * A} * \frac{T_{Std}}{T} \left[\frac{cm^3_{STP}}{m^2\ d}\right] \tag{5}$$

where $\dot{P}_{O_2}$ is the slope of oxygen percentage in the upper chamber against time [hPa s^{-1}], V the volume of the upper chamber [cm^3], A the permeation area [m^2], P_{Std} the standard pressure [hPa], T_{Std} the standard temperature [K], and T the testing temperature [K].

Oxygen permeability ($P(O_2)$) was obtained by Eq. (6).

$$P(O_2) = \frac{OTR}{p^{bulk}_{O_2}} * th \left[\frac{cm^3_{STP}\mu m}{m^2\ d\ Pa}\right] \tag{6}$$

where $p^{bulk}_{O_2}$ is the partial pressure of oxygen in the bulk [Pa] and th the sample thickness [μm].

2.5.3. Optical properties

Optical properties were assessed using a microplate reader (BioTek Synergy H1 Multimode Reader, Agilent, US) equipped with BioTek Take3 plate (Agilent, US). To determine the transparency of the films ($n = 3$ per film type), the percentage of light transmission was measured between 300 and 700 nm, and the light transmission at 660 nm in the visible light range was used to compare the different films (Zhao et al., 2022).

2.6. Provolone cheese coating

For each coating's composition, cylindrical Provolone cheese samples (diameter 1.5 cm, height 1.5 cm, $n = 3$) were used to simulate the actual geometry. The base surfaces of the samples were covered with aluminium foils, so evaporation only occurred on the side surface, thus simulating the typical pear shape of provolone cheese. The samples were then tied with a food-grade thread, dipped in the coating solutions (Table 1) via a custom-made dip coating apparatus (dipping speed = 100 mm min^{-1}), and hung up for coating drying (Fig. S2). In the case of neutralised samples, the $NaOH_{1M}$ neutralisation (30 s dipping) was performed immediately after the dipping phase.

2.7. Characterisation of coated provolone cheese

2.7.1. Cheese weight loss and texture profile analysis

Samples were kept at a storage condition of $T = 3 \pm 1$ °C, RH = 67 ± 10 % for 7 and 14 days and at $T = 23 \pm 1$ °C and RH = 61 ± 3 % for 7 and 14 days to simulate an accelerated storage test. At each time point, thickness, weight loss, and texture profile analyses were performed in triplicate ($n = 3$). The thickness was assessed by cutting the cheese samples into vertical sections and using Scanning Electron Microscopy (EVO 50 EP, ZEISS, Italy). Weight Loss was assessed by weighing the specimens at different time points using Eq. (7).

$$W\ [\%] = \frac{m_i(t) - m_i(t_0)}{m_i(t_0)} \times 100 \tag{7}$$

where W is the mass loss [%], $m_i(t_0)$ the initial mass of the sample + the deposited dry coating [g], and $m_i(t)$ the mass of the sample at time t [g].

Texture profile analysis (TPA) was performed using a uniaxial tensile testing machine (1/MH, MTS) with a 5 kN load cell. The specimens were subjected to a two-step compression up to a deformation of 70 % of their height with a constant crosshead speed of 0.8 mm s^{-1} to simulate the chewing (Peleg, 2019). The generated plot of force (N) vs. time (s) was recorded, and the Hardness (N) and the Chewiness of the samples were investigated. (For more details about TPA parameters determination, please refer to Supporting information and Fig. S3.)

2.7.2. pH of the coating

Before the TPA test, the pH of the surface of the coatings was

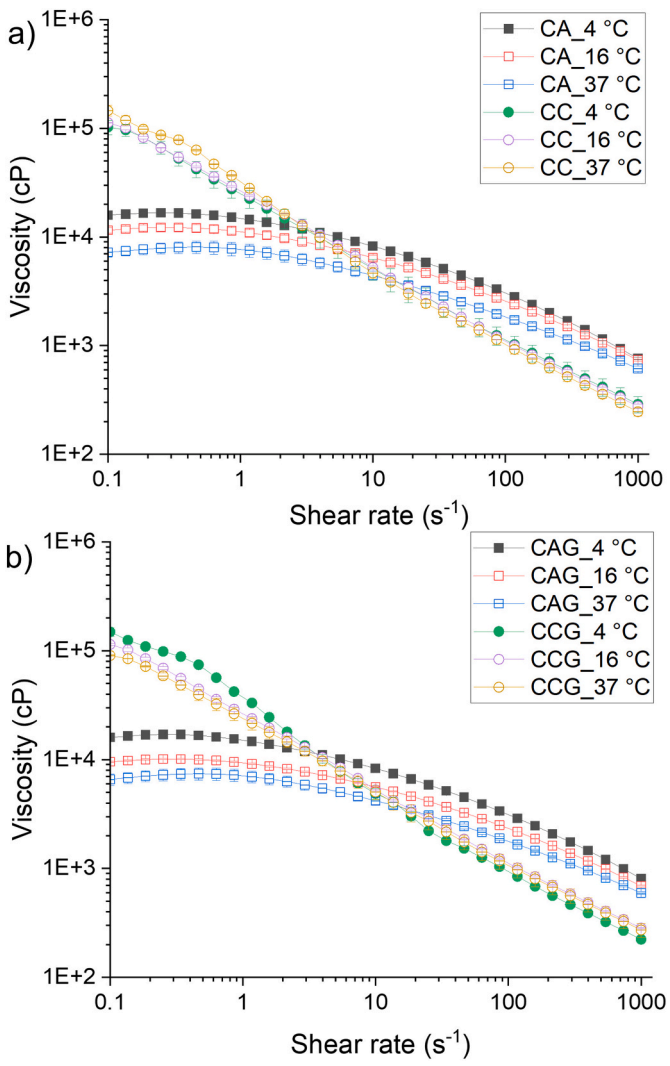

Fig. 1. Viscosity as a function of the shear rates (s^{-1}) at different temperatures. a) Solutions (CA and CC, respectively 4 % w/v and 2 % w/v) without glycerol; b) chitosan solutions after the addition of glycerol (CAG and CCG, respectively 4 % w/v and 2 % w/v).

measured (n = 3 per coating type) with a pH meter (HI5222-02 equipped with a HI1413B electrode, Hanna Instruments Italia s.r.l., Italy), at different time points (0, 7, and 14 days) to estimate residual acetic acid within the coatings.

2.7.3. Analysis of volatile substances

The acetic acid migration analysis within the cheese was carried out by considering the CAG-coated samples after drying at $T = 3 \pm 1$ °C, RH = 67 ± 10 % for 2 and 14 days. The coating was peeled off completely, and the core of the cheese was removed, analysing the external circular crown of the sample (without the coating). The amount of analytes in the acid-coated samples was determined using a gas chromatograph with a Perkin Elmer Clarus 500 MS mass detector coupled with headspace. The identification of migrating species has been conducted through the library "*NIST 2000*".

2.8. Statistical analysis

Unless stated, all tests were carried out in triplicate, and data were expressed as mean (M) ± standard deviation (SD). Statistical analysis was performed using GraphPad Prism 8 (Dotmatics, USA). Comparison among the groups was performed by ANOVA (one-way or two-way) followed by post hoc Tukey's test, with a significance level $\alpha = 0.05$. A *p*-value (p) < 0.05 is reported in the charts with the symbol "*".

3. Results and discussion

3.1. Chitosan solution optimization

Table 1 reports the concentrations of chitosan and acid in the solutions. Concentrations were optimised to trade off the complete chitosan dissolution and the rheological behaviour of the solution for the film casting and dip-coating process. In particular, the residual concentration of acetic acid in the coating must be minimised for food safety and quality.

3.1.1. Rheological characterisation of the chitosan solutions

Fig. 1a-b reports the results of rheological characterisation at 4, 16, and 37 °C, with and without glycerol (10 % w/w_{cs}), performed on the different solutions optimised for the dipping process. The rheological behaviour provides key information for setting and scaling up the dipping process, with typical shear rates in the 10–100 s^{-1} range (Carnicer et al., 2021). The viscosity decreases for all the tested solutions by increasing the shear rate, showing a non-Newtonian (shear thinning) behaviour (El-Hafian et al., 2010). This specific behaviour is advantageous for the dipping process as it facilitates the immersion of the cheese samples.

At a fixed shear rate, the viscosity of acetic acid solutions (CA and CAG) decreases with temperature, especially at lower shear rates, showing an Arrhenius dependence behaviour (Eq. (1)). (Table S1 summarises A and E_a parameters). The solutions prepared with CO_2 (CC and CCG) show negligible dependence on temperature in the studied range (Fig. 1a-b). A higher viscosity of CO_2 solutions (CC and CCG) at lower shear rates and a pronounced shear thinning behaviour is worth noticing. The CCG solution has a lower viscosity at higher shear rates than the CAG solution (Fig. 1), thus facilitating the dipping phase. At the same time, the pronounced shear thinning behaviour led to a rapid increase in viscosity immediately after the dipping phase. This was reflected in a reduced dripping of the coating solution from the samples and a more homogeneous coating on the specimens.

Adding glycerol is expected to reduce the overall viscosity due to its lubricating effect (Prateepchanachai et al., 2017). However, we observed a relevant effect only at low shear rates (0.1 s^{-1}), whereas the plasticizing effect became negligible at higher shear rates. The most significant decrease was observed for CC samples at 37 °C, in which the viscosity at low shear rates (0.1 s^{-1}) decreased significantly by approximately 38 %. At temperatures closer to the dipping conditions, this effect became negligible. In general, the effect of glycerol on solutions containing acetic acid was less pronounced. Despite reducing the viscosity, which may be considered disadvantageous, the glycerol addition is needed to obtain homogeneous and durable coatings. Indeed, the coatings obtained without plasticiser often cracked during the drying step.

3.2. Preparation and characterisation of chitosan films

The effectiveness of coatings is inextricably linked to the attributes of the resulting thin films. The direct measurement of the coating properties, such as permeability, poses significant challenges while studying the material properties, which becomes more feasible when biopolymers are in film form: for this reason, chitosan films were prepared by solvent casting. As a first result, the CO_2 dissolution process eliminated the typical pungent odour of acidic chitosan, resulting in odourless films. Samples of films neutralised with sodium hydroxide were also prepared to remove residual acetic acid completely. NaOH neutralisation is one of the most used treatments to stabilise chitosan films and remove residual acid: $NaOH_{1M}$ treatment (partially) neutralises the residual acid in the film and increases the water stability (Chang et al., 2019; Takara et al.,

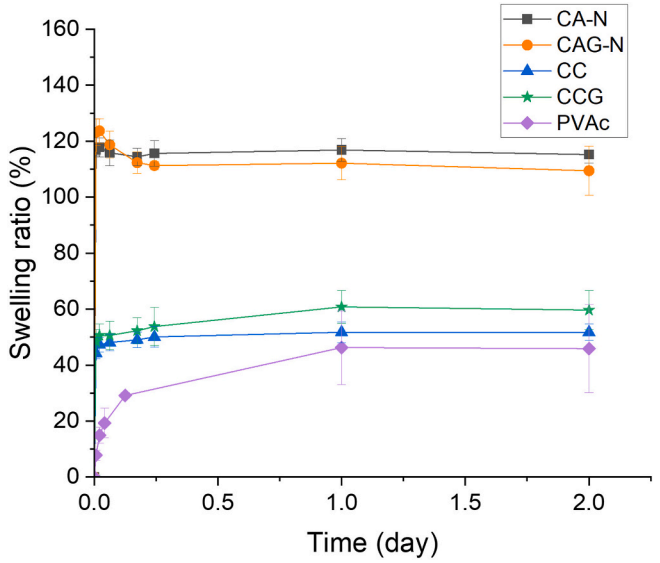

Fig. 2. Swelling ratio of the chitosan-based films in PBS vs. time obtained by casting CA-N (squares), CAG-N (circles), CC (triangles), CCG (stars), and PVAc (rhombuses) solutions.

2015). The contact time was chosen to simulate the time required (30s″) in the dipping phase experiments for a cheese coating application. Due to the short contact time, a high NaOH molarity (1 M) was chosen compared to those found in the literature (Chang et al., 2019; Takara et al., 2015) to ensure a significant neutralisation of the film.

3.2.1. *Water stability of chitosan films*

Developing packaging or coating that must be employed in contact with high-moisture-containing food products requires water stability. For this reason, the swelling ratio of chitosan-based films was first evaluated. Fig. 2 reports the swelling ratio [%] of acid-free films (CC and CCG) compared to acid films after neutralisation with sodium hydroxide (CA-N and CAG-N) and PVAc. The swelling ratio of non-neutralised acidic films is not reported here due to their inherent instability under test conditions. Indeed, once immersed in PBS, they rapidly swell and dissolve in the test solutions; this behaviour was attributed to residual acetic acid in the films.

The CCG films have higher water stability and show a 51 % lower swelling ratio after 2 days than the neutralised films (p-value = 0.0019), which matches the PVAc (p-value = 0.7300). It can be assumed that CO_2 evaporation decreases the charged amino groups on the chitosan chains, which reduces the films' hydrophilicity and enhances intra-chain hydrogen bonding (*i.e.*, increasing physical crosslinking). As an overall result, the kinetic solvation process is significantly slowed down. Adding glycerol (10 % w/w_{cs}) as a plasticiser led to an increased swelling ratio due to its hygroscopic nature. However, the addition of a relatively small amount of this plasticiser limits the worsening effect (p-value CC vs CCG = 0.7989), in good accordance with the literature (Ziani et al., 2008).

As expected, the neutralisation process reduces the swelling ratio compared to non-neutralised ones due to the deprotonation of the amino groups of chitosan after neutralisation. However, some acetic acid molecules, or its salts, may be retained in the film matrix. Indeed, despite the neutralisation step, CA-N and CAG-N samples showed a higher swelling ratio compared to acid-free films (CC and CCG) and, consequently, lower stability in aqueous environment. To overcome this issue, the contact time, or the molarity of NaOH, could be increased to achieve complete AcOH neutralisation. However, previous studies showed that longer neutralisation times did not further reduce the swelling rate of chitosan films at low NaOH concentrations (0.25 M and 1.25 M). At a higher NaOH concentration (2.5 M), the neutralisation rate increased significantly, resulting in greater resistance to swelling (Chang et al., 2019; Takara et al., 2015). However, it can leave NaOH residues in the films, which are detrimental in food coating applications.

To better visualise these results, CCG, CAG, and CAG-N films were exposed to hot water vapour (80 °C) for 3 h, and pictures were collected every 20 min. While CAG and CAG-N films swell and deform after the first minutes, the CCG film remains stable for all the experiments (see Supplementary materials for details). From an applicative point of view, acid-free solutions optimise water stability in chitosan films by avoiding the complexity of a dual-stage process in strong alkaline baths.

3.2.2. *Water vapour and oxygen permeability*

Water and oxygen permeabilities are essential in effectively selecting materials for food coatings. To our knowledge, no characterisations exist in the literature for acid-free chitosan-based films.

Fig. 3a summarises the water vapour permeability of the developed films. It can be observed that the neutralisation of acidic films (CAG-N) leads to a lower WVP (0.017 ± 0.002 g mm m^{-2} d^{-1} Pa^{-1}), which correlates with the higher water stability compared to non-neutralised chitosan (CAG, 0.022 ± 0.002 g mm m^{-2} d^{-1} Pa^{-1}). This could be caused by the decreased interchain distance between chitosan molecules

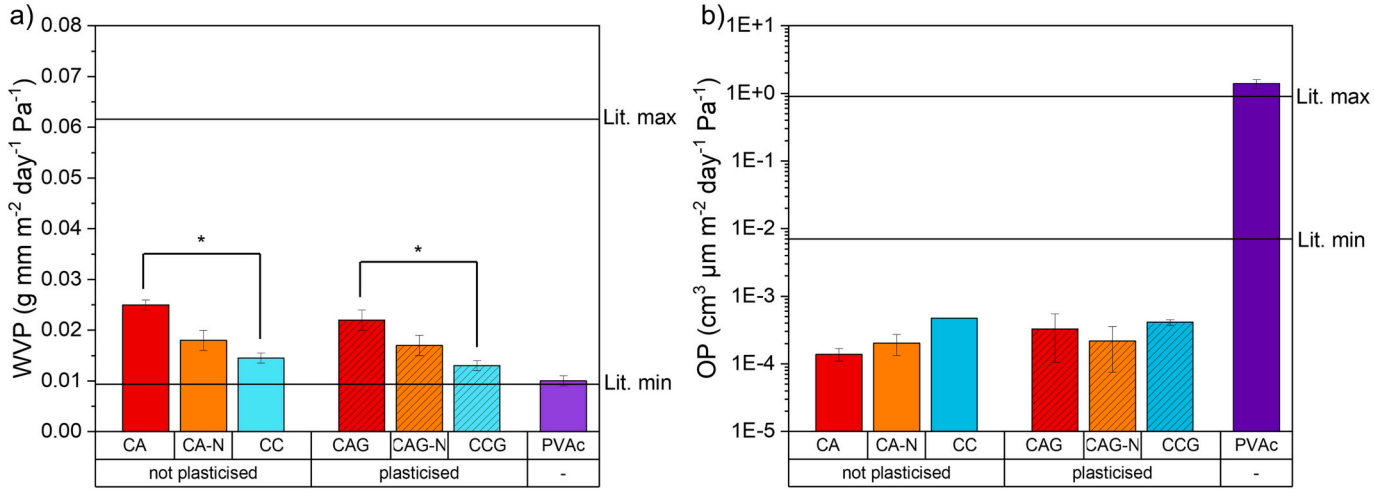

Fig. 3. a) Water vapour permeabilities (WVP) of chitosan-based films. The lines "Lit. Min" and "Lit. Max" are the minimum and maximum WVP values reported in the literature (V. & Badwaik, 2022; Cazón et al., 2017; Cazón & Vázquez, 2020) b) oxygen permeability of chitosan-based films. The lines "Lit. Min" and "Lit. Max" are the minimum and maximum OP values reported in the literature (Cazón et al., 2017; Cazón & Vázquez, 2020; Yousuf et al., 2018).

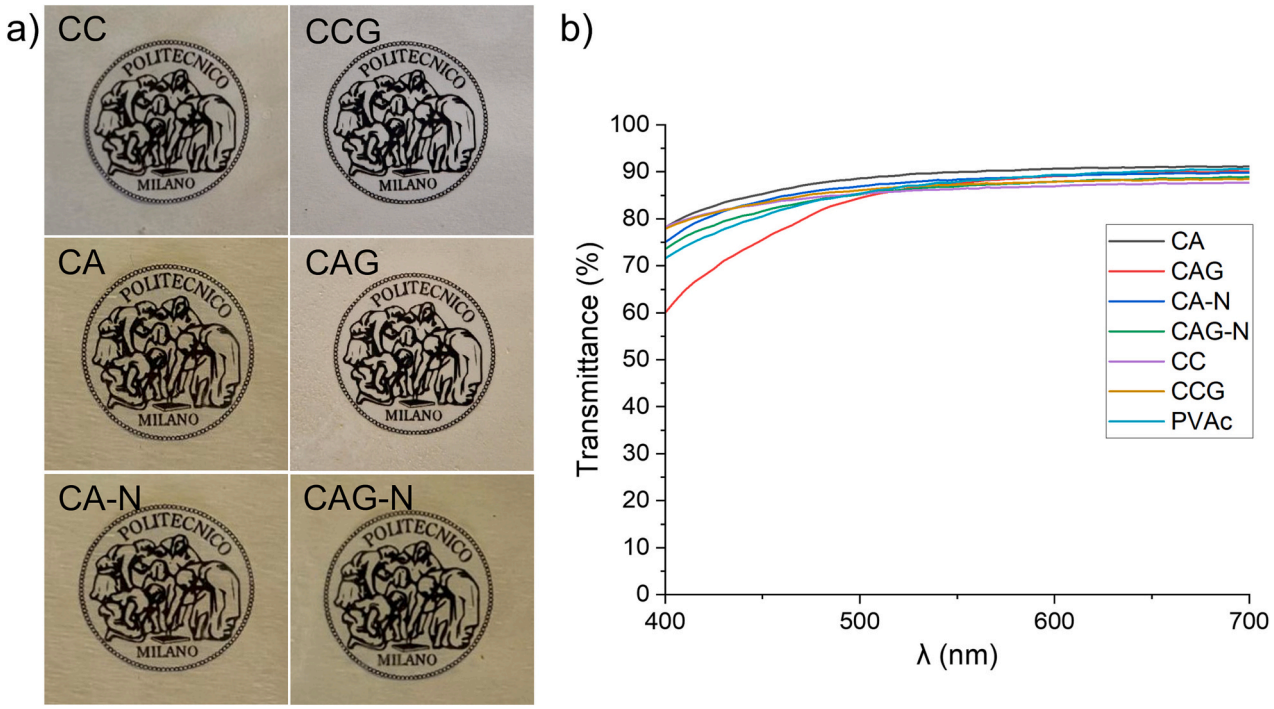

Fig. 4. a) Transparency of chitosan films, b) transmittance of the different films compared to PVAc.

after removing acetic acid (Chang et al., 2019; Xu et al., 2022). The acid-free film (CCG), which shows the best water stability, also resulted in the lowest WVP (0.013 ± 0.001 g mm m^{-2} d^{-1} Pa^{-1}), achieving a significant improvement compared to CAG (p-value = 0.0007) and matching the performance of CAG-N (p-value = 0.1970) and PVAc (0.010 ± 0.001 g mm m^{-2} d^{-1} Pa^{-1}) (p-value = 0.0714) (Table S2).

The barrier to moisture in chitosan films, and polysaccharides in general, is very low (Ruggeri et al., 2021). This fact is attributed to its hydrophilic nature, which allows water molecules to interact with the matrix, thus increasing their permeation rate (Jiménez-Gómez & Cecilia, 2020). The addition of glycerol in small amounts appears to improve the water barrier of chitosan films, although not significantly, which is in agreement with results obtained in other studies (Rivero et al., 2016). However, as reported by Cerqueira et al. (Cerqueira et al., 2012), adding glycerol in quantity higher than 20–30 % w/w_{cs} should increase water vapour permeability. The addition of plasticiser increases the free volume and polymer chain mobility, resulting in a higher water vapour diffusion. For this reason, a higher amount of glycerol was not considered (Cerqueira et al., 2012; Rivero et al., 2016). By removing the acid and adding a small amount of glycerol, the acid-free solution (CCG) matches the performance of PVAc-based films.

Fig. 3b compares the oxygen barrier properties of the different film formulations. No significant differences can be observed between CCG, CAG-N, and CAG ($P(O_2) = 4.1 \pm 0.4$, 2.2 ± 1.4, and $3.3 \pm 2.2 \times 10^{-4}$ cm^3 μm m^{-2} d^{-1} Pa^{-1}, respectively). This data aligns with the range of values commonly found in the literature (Cazón et al., 2017; Cazón & Vázquez, 2020; Yousuf et al., 2018) (further data are collected in Table S3). The lower standard deviation in the case of acid-free films suggests a better homogeneity of these samples than acid-based films. At the same time, a significant improvement in oxygen permeability is obtained compared to PVAc (more than three orders of magnitude).

3.2.3. Optical properties

Preserving the quality of cheese is essential, hinging on the protection against UV light can trigger various undesirable reactions, leading to food product deterioration and a notable decline in shelf life and quality. As a result, the optical attributes of coating materials, encompassing UV–vis absorbance and transparency, not only hold strategic importance but also influence consumer acceptance significantly (Jafarzadeh et al., 2021). Indeed, considering that the transparency of a food coating is generally a feature appreciated by the consumer, the optical properties of the films were studied in terms of light transmission in the 400–700 nm range. All the films are characterised by high transparency in the visible spectrum range (Fig. 4). At λ = 660 nm, CCG film displayed a transmittance of 88 %, comparable to CAG (90 %) and CAG-N (89 %). Notably, the transparency values of the films with chitosan did not significantly differ from the PVAc film (90 %). In particular, the CCG results in a transparent and homogeneous film (Fig. 4a); moreover, adding glycerol does not affect the film's transparency, as in CC and CCG (Fig. 4a-b). Generally, CC and CCG films exhibit less yellowish tint when compared to their counterparts produced using acetic acid.

3.3. Cheese coatings

Cylindrical samples of provolone cheese were dipped in a chitosan solution at room temperature, whose composition was tuned to achieve an optimal viscosity, making the dipping process efficient and limiting the dripping effect. The geometry of the samples was designed to simulate the geometry of provolone cheese as closely as possible. In addition, to simulate the geometry of the whole provolone cheese, the two-cylinder bases were sealed by applying two circular aluminium foils, thus limiting the transport phenomena between cheese, coating, and environment only to the side surfaces of the samples. After the dipping stage, the coated samples were allowed to dry to form a coating film on the cheese samples. During the drying step, coatings prepared with CC and CA solutions (*i.e.*, not containing glycerol) appear inhomogeneous and tend to crack, resulting in samples that cannot be considered satisfactory for the proposed application. For this reason, only results from plasticised coatings will be discussed in the following section.

3.3.1. Coating appearance and thickness

After dipping, part of the wet coating is dripped along the cheese

Table 2
The thickness of different coatings after dipping.

Coating	Sample weight [g]	Wet coating [g]	Dry coating [g]	Thickness [μm]
CAG	7.268 ± 0.074	1.129 ± 0.122	0.049 ± 0.005	45 ± 11
CAG-N	7.361 ± 0.392	2.458 ± 0.475	0.108 ± 0.021	75 ± 7
CCG	7.158 ± 0.278	4.815 ± 1.193	0.106 ± 0.026	76 ± 4
PVAc	7.269 ± 0.089	1.184 ± 0.185	0.532 ± 0.093	90 ± 12

samples, affecting the amount of deposited solution. The CCG solution does not exhibit this phenomenon (Fig. S2), probably due to the higher viscosity and the pronounced shear-thinning behaviour. On the contrary, acidic solutions showed a wide dripping due to the lower viscosity, resulting in a non-homogeneous coating adhesion to the cheese.

Table 2 compares the final thickness after drying, measured by SEM (Fig. 5). The acid-free films are thicker than the CAG solution (p-value = 0.0015, Fig. 5a) despite the chitosan solution concentration being half of the other solutions. This is a direct result of the shear-thinning behaviour observed in the CC and CCG solutions. The higher thickness was noticeable on samples where the solution did not drip during drying. Most of the CAG and PVAc solutions (dry matter = 45 %), due to their low viscosity (η (25 °C) = 200–800 cP), accumulate at the base of the sample, where thickness measure has not been assessed (Fig. 5c, d). CCG coating possesses thickness which does not significantly differ from PVAc (p-value = 0.0738), indicating that this approach can be exploited to replace state-of-the-art solutions. From a thickness point of view, CAG-N coating does not significantly differ from PVAc (p-value = 0.0878). However, the extra dipping steps required for the neutralisation and the other drawbacks described above make this approach unsustainable. It is worth noticing that the results for the thickness of CAG (Table 2) are in accordance with similar chitosan solutions tested in other studies, which reported a thickness of 66 μm for dipping Mozzarella cheese (Zhong et al., 2014). Fig. 5b shows that $NaOH_{1M}$ treatment resulted in thicker coatings than without treatment, achieving a 69–85 μm thickness.

3.3.2. *Weight loss and texture profile analysis*

Fig. 6 and Tables S4-S5 report the weight loss of coated cheese at two different temperatures (T = 3 ± 1 °C, RH = 67 ± 10 % and T = 23 ± 1 °C, RH = 61 ± 3 %) for 14 days: all the coatings provide a barrier to water evaporation, with differences more evident at T = 23 °C. The neutralised (CAG-N) and acid-free (CCG) coated samples show the lowest weight loss, compared to the uncoated control, at 7 (p-value = 0.0196; p-value = 0.0044) and 14 days at 23 °C (p-value = 0.0370; p-value = 0.0119). This trend can be correlated to the higher coating thickness (Table 2) and the lower water vapour permeability (Fig. 3). Moreover, both coatings match the PVA-based coating performance (p-value >0.5). It is worth noting that, when stored at T = 23 °C, some liquid droplets can be observed on the cheese sample surface. As discussed earlier, CAG coatings are less stable towards hydration; consequently, a noticeable degree of swelling in the CAG coating can be observed macroscopically, leading to partial degradation of the acid-containing films, reflected in the weight loss data. After 7 days, the difference in the weight loss with the uncoated control becomes negligible (p-value = 0.7277).

Fig. 6b shows the test performed at a lower temperature (T = 3 ± 1 °C; RH = 67 ± 10 %): CCG coating achieved a significant improvement in weight loss prevention compared to CAG and uncoated control until 7 days (p-value = 0.0003; p-value <0.0001). It is also crucial to underline that all the coatings maintain significance in weight loss prevention compared to the uncoated control after 14 days (p-value <0.05).

Weight loss due to the rapid dehydration of the product is a crucial parameter for preserving cheese's texture and organoleptic properties

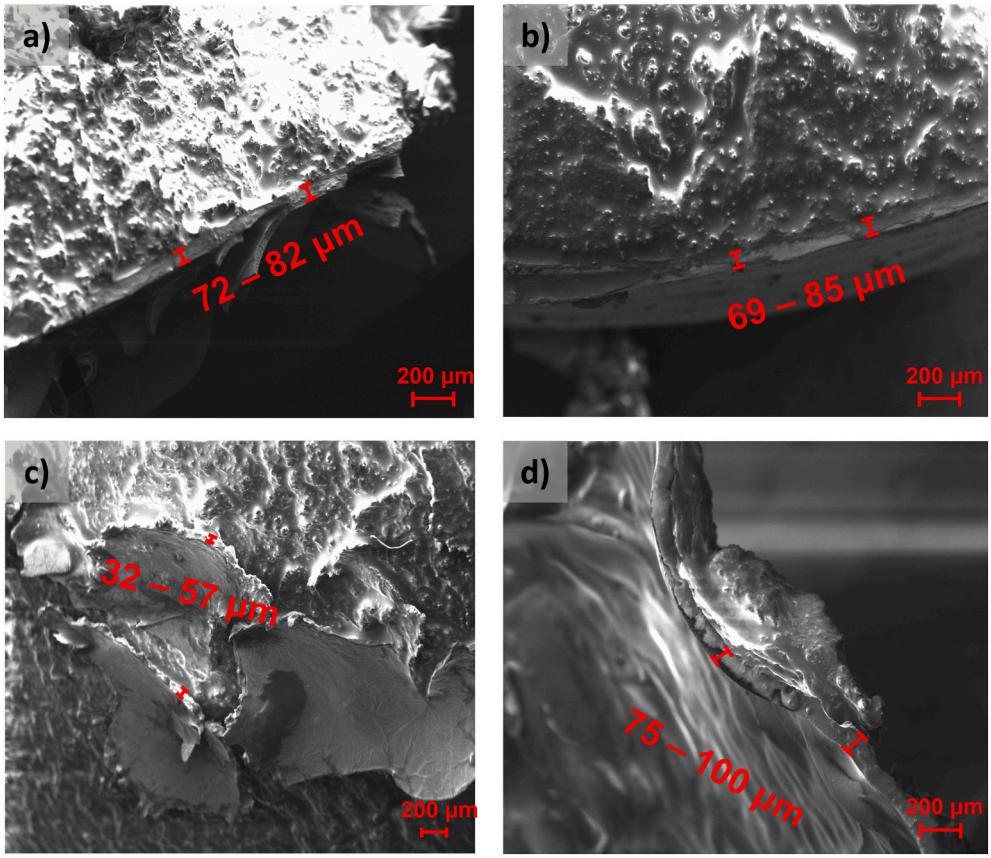

Fig. 5. SEM micrographs of Provolone cheese cross-section with a different coating. a) CCG b) CAG-N c) CAG d) PVAc (scalebar = 200 μm).

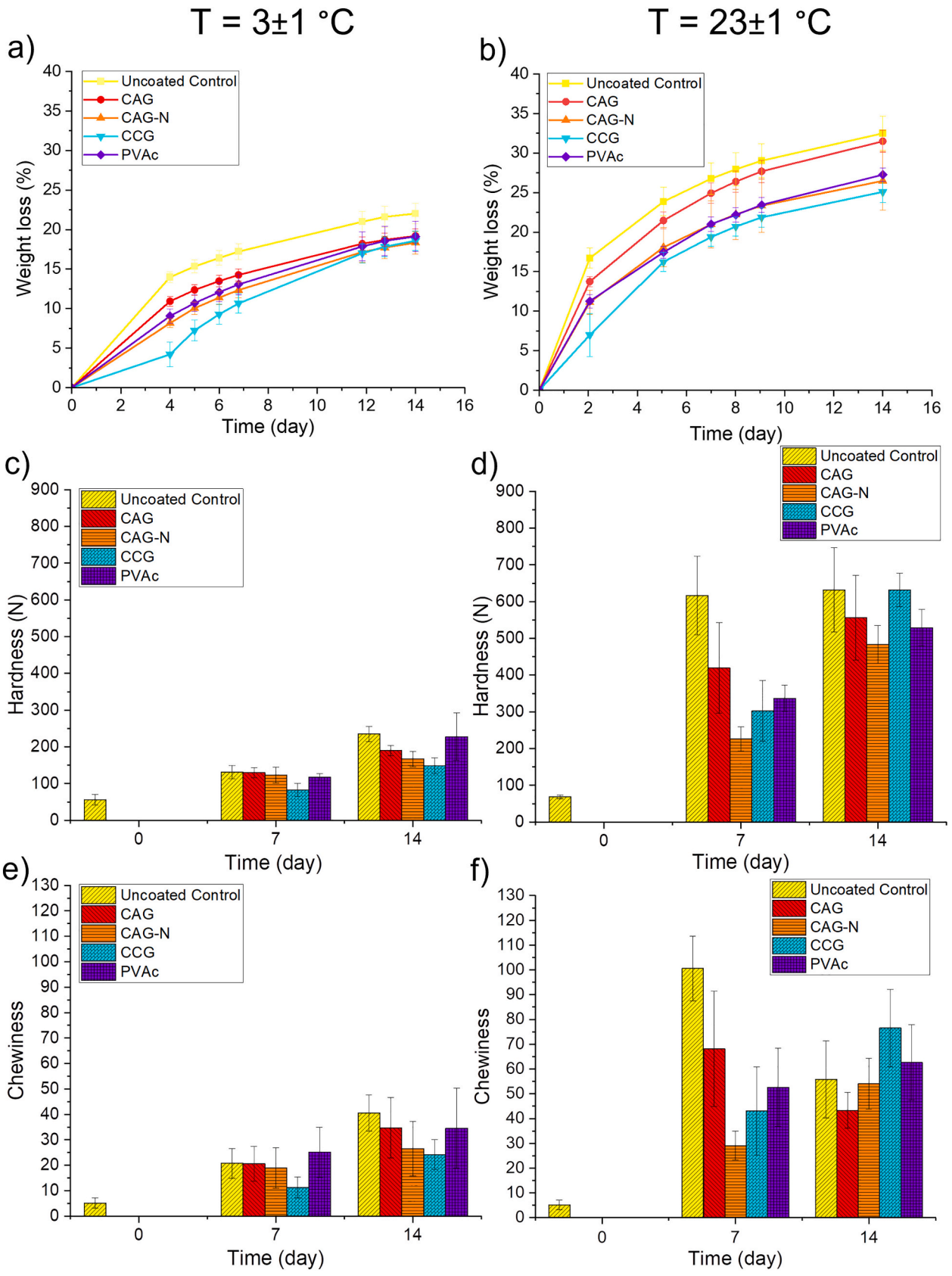

Fig. 6. Weight loss (%) over time of coated and uncoated samples at a) $T = 3 \pm 1$ °C; RH = 67 ± 10 % and b) T = 23 ± 1 °C; RH = 61 ± 3 %. Results of TPA on coated and uncoated Provolone cheese samples after 7 and 14 days at c), e) T = 3 ± 1 °C; RH = 67 ± 10 % and d), f) T = 23 ± 1 °C; RH = 61 ± 3 %.

Table 3
Acetic acid content from GC–MS-HS analysis on CAG coated samples after drying (T = 3 ± 1 °C; RH = 67 ± 10 %).

Sample	Mass [g]	Acetic acid content [mg]	Acetic acid content [ppm]
Uncoated control	1.88 ± 0.2	0	0
CAG (2 days drying)	2.55 ± 0.16	0–0.22	0–93
CAG (14 days drying)	1.96 ± 0.1	0.16–0.26	77–140
CAG-N (2 days drying)	2.04 ± 0.4	0.15–0.25	61–124
CAG-N (14 days drying)	1.58 ± 0.2	0.18–0.29	116–209

(Jafarzadeh et al., 2021). A texture profile analysis (TPA) was carried out after up to 14 days at the two storage conditions (Fig. 6c-d-e-f and Tables S6-S7). Hardness, cohesiveness, and springiness can be obtained from the test to calculate chewiness as the product of the three parameters (see Supplementary Materials), which simulates the resistance of the sample during chewing (Allen Foegeding et al., 2003). The higher this value, the harder the cheese will be to chew. One parameter that changes most after 7 days of storage is the hardness at 23 °C and 4 °C (Fig. 6c-d). It was highlighted that coatings that better protected against dehydration during storage preserve the inner softness of the cheese. Based on the chewiness comparison (Fig. 6e-f), it is evident that the acid-neutralised and acid-free coatings are the most effective in preserving the texture of Provolone cheese after 7 days of storage under different conditions. This is due to their superior moisture barrier properties, which help to reduce water evaporation from the cheese and result in a significant improvement compared to the uncoated control. Additionally, the acid-neutralised and acid-free coatings were found to perform as well as PVAc in terms of texture preservation.

3.3.3. Acetic acid migration

The pH of the coating was measured in the samples at T = 3 ± 1 °C for up to 14 days (Fig. S4) to evaluate the residual acetic acid in the coating that may migrate in coated cheese. CAG coating shows an acidic pH up to 7 days, suggesting some residual acetic acid within the coating. After 14 days, a higher pH was detected, indicating the possibility that the acetic acid migrated into the samples or evaporated. The acetic acid content in the cheese layer underneath the coating was measured to confirm this hypothesis using GC–MS-HS analysis (Figs. S5, S6, S7, S8, and S9). Table 3 summarises the range of acetic acid migrated in the provolone cheese up to 14 days.

A non-negligible migration of acetic acid from the coating to the cheese matrix is evident, even in NaOH-neutralised samples. This confirms the hypothesis that some acetic acid molecules, or their salts, are retained in the film matrix, causing low water stability 3.2.1 (Fig. 2). In CAG-coated samples, the migrated acetic acid content results higher than the specific migration limit of 60 ppm for food contact materials (Reg 10/2011 EU, 2011), especially after 14 days of storage (77–140 ppm). However, considering a 1 kg Provolone cheese, assuming cylindrical shape (diameter = 13 cm; height = 10 cm), it is possible to estimate the migration of acetic acid for a real dipping case (0–26 ppm, after 2 days; 18–30 ppm, after 14 days). The acetic acid content reported in a real provolone scenario meets the specific migration limit (60 ppm). However, having a strong and pungent odour and taste, acetic acid would irreparably compromise the quality and the organoleptic properties of the cheese product, exciding the odour detection limit range of acetic acid reported by the literature (0.006–0.135 ppm) (Nagata, 2012; Vera et al., 2020). Similar considerations can be made for NaOH-neutralised samples (CAG-N). The migration data, reported in Table 3, highlight that the acetic acid content is even higher than CAG; this can be attributed to the increased amount of coating solution adhering to the specimens, leading to increased coating thickness. Overall, the coating neutralisation step is inefficient in removing acidic residues in compliance with food quality and safety regulations.

4. Conclusion

This study introduces a novel method for producing chitosan coatings suitable for food applications without utilizing acetic acid. The process involves modifications to a prior method that allows the dissolving of chitosan in carbonated deionised water. To test the effectiveness of this acid-free chitosan as a food coating, Provolone cheese, a traditional Italian food product, was used as a model. A comprehensive understanding of the overall behaviour of the obtained coating has been gained by integrating a characterisation from the chitosan solution to the final food product.

Viscosity measurement showed a strong shear thinning behaviour, facilitating the immersion of the cheese samples and reducing the coating solution's dripping from the samples, resulting in more homogeneous coatings. The acid-free chitosan films have superior water stability and barrier properties compared to commonly acetic acid ones. When applied to Provolone cheese, acid-free chitosan coatings showed the ability to preserve cheese properties comparable to commercial PVAc and chitosan film from conventional aqueous acetic acid. Still, it was demonstrated that the residual acid in acetic acid-processed chitosan exceeded the specific migration limit for packaging in contact with food and the odour detection limit, compromising the organoleptic properties of the cheese and deteriorating its quality.

In conclusion, processing chitosan via wet approaches that eliminate acetic acid has been proven to be a promising alternative to conventional dissolution. This method further enhances the properties of chitosan films. It enables them to meet stringent food quality requirements and safety regulations, paving the way for an effective application of chitosan in future food contact applications.

CRediT authorship contribution statement

Roberto Casalini: Writing – original draft, Methodology, Investigation, Data curation. **Filippo Ghisoni:** Writing – review & editing, Investigation. **Lorenzo Bonetti:** Writing – review & editing, Methodology, Investigation. **Andrea Fiorati:** Writing – review & editing, Writing – original draft, Methodology, Formal analysis, Data curation, Conceptualization. **Luigi De Nardo:** Writing – review & editing, Supervision, Funding acquisition, Formal analysis, Conceptualization.

Declaration of competing interest

The authors declare the following financial interests/personal relationships which may be considered as potential competing interests:

Fiorati Andrea, Luigi De Nardo reports financial support was provided by European Union Next-GenerationEU PNRR MISSIONE 4 COMPONENTE 2 INVESTIMENTO 1 4 - DD 1032 17-06-2022 CN00000022 and MISSIONE 4 COMPONENTE 2 INVESTIMENTO 1 3 - DD 1551 11-10-2022 PE00000004.

Data availability

Data will be made available on request.

Acknowledgements

The authors acknowledge that this study was partially conducted within the Agritech National Research Center and received funding from the European Union Next-GenerationEU (PIANO NAZIONALE DI RIPRESA E RESILIENZA (PNRR) – MISSIONE 4 COMPONENTE 2, INVESTIMENTO 1.4 – D.D. 1032 17/06/2022, CN00000022), and within the MICS (Made in Italy – Circular and Sustainable) Extended Partnership and received funding from the European Union Next-GenerationEU (PIANO NAZIONALE DI RIPRESA E RESILIENZA (PNRR) – MISSIONE 4 COMPONENTE 2, INVESTIMENTO 1.3 – D.D. 1551.11-10-2022, PE00000004). This manuscript reflects only the authors' views and opinions. Neither the European Union nor the European Commission can be considered responsible for them.

Appendix A. Supplementary data

Supplementary data to this article can be found online at https://doi.org/10.1016/j.carbpol.2024.121842.

References

Allen Foegeding, E., Brown, J., Drake, M., & Daubert, C. R. (2003). Sensory and mechanical aspects of cheese texture. *International Dairy Journal, 13*(8), 585–591. https://doi.org/10.1016/S0958-6946(03)00094-3

Amulya, K., Katakojwala, R., Ramakrishna, S., & Venkata Mohan, S. (2021). Low carbon biodegradable polymer matrices for sustainable future. *Composites Part C: Open Access, 4*, Article 100111. https://doi.org/10.1016/j.jcomc.2021.100111

Cano Embuena, A. I., Cháfer Nácher, M., Chiralt Boix, A., Molina Pons, M. P., Borrás Llopis, M., Beltran Martínez, M. C., & González Martínez, C. (2017). Quality of goat's milk cheese as affected by coating with edible chitosan-essential oil films. *International Journal of Dairy Technology, 70*(1), 68–76. https://doi.org/10.1111/1471-0307.12306

Carnicer, V., Alcázar, C., Orts, M. J., Sánchez, E., & Moreno, R. (2021). Microfluidic rheology: A new approach to measure viscosity of ceramic suspensions at extremely high shear rates. *Open Ceramics, 5*, Article 100052. https://doi.org/10.1016/j.oceram.2020.100052

Cazòn, P. (2017). Polysaccharide-basedfilms and coatings for food packaging: A review. *Food Hydrocolloids, 1–13*. doi:.1037//0033-2909.I26.1.78.

Cazón, P., & Vázquez, M. (2020). Mechanical and barrier properties of chitosan combined with other components as food packaging film. *Environmental Chemistry Letters, 18*(2), 257–267. https://doi.org/10.1007/s10311-019-00936-3

Cazón, P., Velazquez, G., Ramírez, J. A., & Vázquez, M. (2017). Polysaccharide-based films and coatings for food packaging: A review. *Food Hydrocolloids, 68*, 136–148. https://doi.org/10.1016/j.foodhyd.2016.09.009

Cerqueira, M. A., Souza, B. W. S., Teixeira, J. A., & Vicente, A. A. (2012). Effect of glycerol and corn oil on physicochemical properties of polysaccharide films – A comparative study. *Food Hydrocolloids, 27*(1), 175–184. https://doi.org/10.1016/j.foodhyd.2011.07.007

Chang, W., Liu, F., Sharif, H. R., Huang, Z., Goff, H. D., & Zhong, F. (2019). Preparation of chitosan films by neutralization for improving their preservation effects on chilled meat. *Food Hydrocolloids, 90*, 50–61. https://doi.org/10.1016/j.foodhyd.2018.09.026

El-Hafian, E. A., Elgannoudi, E. S., Mainal, A., & Yahaya, A. H. B. (2010). Characterization of chitosan in acetic acid: Rheological and thermal studies. *Turkish Journal of Chemistry*. https://doi.org/10.3906/kim-0901-38

Elsabee, M. Z., & Abdou, E. S. (2013). Chitosan based edible films and coatings: A review. *Materials Science and Engineering: C, 33*(4), 1819–1841. https://doi.org/10.1016/j.msec.2013.01.010

Fox, P. F., Guinee, T. P., Cogan, T. M., & McSweeney, P. L. H. (2017). Principal families of cheese. In *Fundamentals of cheese science* (pp. 27–69). Springer US. https://doi.org/10.1007/978-1-4899-7681-9_3.

Gennadios, A., Hanna, M. A., & Kurth, L. B. (1997). Application of edible coatings on meats, poultry and seafoods: A review. *LWT - Food Science and Technology, 30*(4), 337–350. https://doi.org/10.1006/fstl.1996.0202

Gorczyca, G., Tylingo, R., Szweda, P., Augustin, E., Sadowska, M., & Milewski, S. (2014). Preparation and characterization of genipin cross-linked porous chitosan–collagen–gelatin scaffolds using chitosan–CO2 solution. *Carbohydrate Polymers, 102*, 901–911. https://doi.org/10.1016/j.carbpol.2013.10.060

Iqbal, M. W., Riaz, T., Yasmin, I., Leghari, A. A., Amin, S., Bilal, M., & Qi, X. (2021). Chitosan-based materials as edible coating of cheese: A review. *Starch - Stärke, 73*(11–12). https://doi.org/10.1002/star.202100088

Jafarzadeh, S., Salehabadi, A., Mohammadi Nafchi, A., Oladzadabbasabadi, N., & Jafari, S. M. (2021). Cheese packaging by edible coatings and biodegradable nanocomposites; improvement in shelf life, physicochemical and sensory properties. *Trends in Food Science & Technology, 116*, 218–231. https://doi.org/10.1016/j.tifs.2021.07.021

Jiménez-Gómez, C. P., & Cecilia, J. A. (2020). Chitosan: A natural biopolymer with a wide and varied range of applications. *Molecules, 25*(17), 3981. https://doi.org/10.3390/molecules25173981

Kocira, A., Kozłowicz, K., Panasiewicz, K., Staniak, M., Szpunar-Krok, E., & Hortyńska, P. (2021). Polysaccharides as edible films and coatings: Characteristics and influence on fruit and vegetable quality—A review. *Agronomy, 11*(5), 813. https://doi.org/10.3390/agronomy11050813

Mohamed, S. A. A., El-Sakhawy, M., & El-Sakhawy, M. A. M. (2020). Polysaccharides, protein and lipid-based natural edible films in food packaging: A review. In. *Carbohydrate Polymers*. https://doi.org/10.1016/j.carbpol.2020.116178

Nagata, Y. (2012). Measurement of odor threshold value review of "Measurement of threshold value by tiriangle odor bag method (Bull. Jap. Env. Sanit. Cent. No. 17. 1990)" paper. *Journal of Japan Association on Odor Environment, 43*(6), 401–407. https://doi.org/10.2171/jao.43.401

Novikov, I. V., Pigaleva, M. A., Abramchuk, S. S., Molchanov, V. S., Philippova, O. E., & Gallyamov, M. O. (2018). Chitosan composites with Ag nanoparticles formed in carbonic acid solutions. *Carbohydrate Polymers, 190*, 103–112. https://doi.org/10.1016/j.carbpol.2018.02.076

Otake, K., Shimomura, T., Goto, T., Imura, T., Furuya, T., Yoda, S., … Abe, M. (2006). One-step preparation of chitosan-coated cationic liposomes by an improved supercritical reverse-phase evaporation method. *Langmuir, 22*(9), 4054–4059. https://doi.org/10.1021/la051662a

Otoni, C. G., Avena-Bustillos, R. J., Azeredo, H. M. C., Lorevice, M. V., Moura, M. R., Mattoso, L. H. C., & McHugh, T. H. (2017). Recent advances on edible films based on fruits and vegetables—A review. *Comprehensive Reviews in Food Science and Food Safety, 16*(5), 1151–1169. https://doi.org/10.1111/1541-4337.12281

Paulo, A. F. S., Baú, T. R., Ida, E. I., & Shirai, M. A. (2021). Edible coatings and films with incorporation of prebiotics—A review. *Food Research International, 148*, Article 110629. https://doi.org/10.1016/j.foodres.2021.110629

Peleg, M. (2019). The instrumental texture profile analysis revisited. *Journal of Texture Studies, 50*(5), 362–368. https://doi.org/10.1111/jtxs.12392

Prateepchanachai, S., Thakhiew, W., Devahastin, S., & Soponronnarit, S. (2017). Mechanical properties improvement of chitosan films via the use of plasticizer, charge modifying agent and film solution homogenization. *Carbohydrate Polymers, 174*, 253–261. https://doi.org/10.1016/j.carbpol.2017.06.069

Rao, L. (2023). Recent trends in biodegradable packaging of foods and food products. In *Food process engineering and technology* (pp. 215–232). Springer Nature Singapore. https://doi.org/10.1007/978-981-99-6831-2_11.

Reg 10/2011 EU. (2011). COMMISSION REGULATION (EU) No 10/2011 of 14 January 2011 on plastic materials and articles intended to come into contact with food.

Rivero, S., Damonte, L., García, M. A., & Pinotti, A. (2016). An insight into the role of glycerol in chitosan films. *Food Biophysics, 11*(2), 117–127. https://doi.org/10.1007/s11483-015-9421-4

Ruggeri, E., Farè, S., De Nardo, L., & Marelli, B. (2021). Edible biopolymers for food preservation. In *Sustainable food packaging technology* (pp. 57–105). Wiley. https://doi.org/10.1002/9783527820078.ch3.

Sakai, Y., Hayano, K., Yoshioka, H., Fujieda, T., Saito, K., & Yoshioka, H. (2002). Chitosan-coating of cellulosic materials using an aqueous chitosan-CO2 solution. *Polymer Journal, 34*(3), 144–148. https://doi.org/10.1295/polymj.34.144

Sakai, Y., Hayano, K., Yoshioka, H., & Yoshioka, H. (2001). A novel method of dissolving chitosan in water for industrial application. *Polymer Journal, 33*(8), 640–642. https://doi.org/10.1295/polymj.33.640

Takara, E. A., Marchese, J., & Ochoa, N. A. (2015). NaOH treatment of chitosan films: Impact on macromolecular structure and film properties. *Carbohydrate Polymers, 132*, 25–30. https://doi.org/10.1016/j.carbpol.2015.05.077

V., A., & Badwaik, L. S. (2022). Recent advancement in improvement of properties of polysaccharides and proteins based packaging film with added nanoparticles: A review. *International Journal of Biological Macromolecules, 203*, 515–525. https://doi.org/10.1016/j.ijbiomac.2022.01.181

Vera, P., Canellas, E., & Nerín, C. (2020). Compounds responsible for off-odors in several samples composed by polypropylene, polyethylene, paper and cardboard used as food packaging materials. *Food Chemistry, 309*, Article 125792. https://doi.org/10.1016/j.foodchem.2019.125792

Warmke, R., Belitz, H.-D., & Grosch, W. (1996). Evaluation of taste compounds of Swiss cheese (Emmentaler). *Zeitschrift für Lebensmittel-Untersuchung und -Forschung, 203*(3), 230–235. https://doi.org/10.1007/BF01192869

Xu, J., Liu, K., Chang, W., Chiou, B.-S., Chen, M., & Liu, F. (2022). Regulating the physicochemical properties of chitosan films through concentration and neutralization. *Foods, 11*(11), 1657. https://doi.org/10.3390/foods11111657

Yousuf, B., Qadri, O. S., & Srivastava, A. K. (2018). Recent developments in shelf-life extension of fresh-cut fruits and vegetables by application of different edible coatings: A review. *LWT, 89*, 198–209. https://doi.org/10.1016/j.lwt.2017.10.051

Zhang, C. J., Liu, Y., Zhang, L., Wang, H. F., & Zhu, P. (2018). Dissolution and regeneration behavior of chitosan in CO $_2$ aqueous solution. *Integrated Ferroelectrics, 189*(1), 24–35. https://doi.org/10.1080/10584587.2018.1454793

Zhao, J., Wang, Y., & Liu, C. (2022). Film transparency and opacity measurements. *Food Analytical Methods, 15*(10), 2840–2846. https://doi.org/10.1007/s12161-022-02343-x

Zhong, Y., Cavender, G., & Zhao, Y. (2014). Investigation of different coating application methods on the performance of edible coatings on Mozzarella cheese. *LWT - Food Science and Technology, 56*(1), 1–8. https://doi.org/10.1016/j.lwt.2013.11.006

Ziani, K., Oses, J., Coma, V., & Maté, J. I. (2008). Effect of the presence of glycerol and Tween 20 on the chemical and physical properties of films based on chitosan with different degree of deacetylation. *LWT - Food Science and Technology, 41*(10), 2159–2165. https://doi.org/10.1016/j.lwt.2007.11.023